

5-14-2019

Suppression of Electron Yield With Carbon Nanotube Forests: A Case Study

Brian Wood
Utah State University

Jordan Lee
Utah State University

Gregory Wilson
National Technical Systems

T.-C. Shen
Utah State University

JR Dennison
Utah State University

Follow this and additional works at: https://digitalcommons.usu.edu/mp_conf

 Part of the [Condensed Matter Physics Commons](#)

Recommended Citation

Brian Wood, Jordan Lee, Gregory Wilson, T.C. Shen and JR Dennison, "Suppression of Electron Yields with Carbon Nanotube Forests: A Case Study," Proceedings of the Applied Space Environments Conference 2019, (Los Angeles, CA, May 12-17, 2019).

This Presentation is brought to you for free and open access by the Materials Physics at DigitalCommons@USU. It has been accepted for inclusion in Conference Proceedings by an authorized administrator of DigitalCommons@USU. For more information, please contact digitalcommons@usu.edu.

Suppression of Electron Yield with Carbon Nanotube Forests: A Case Study

Brian Wood¹, Jordan Lee¹, Gregory Wilson², T.-C. Shen¹, and JR Dennison¹

¹Utah State University, Logan, UT, 84321, USA (e-mail: brian.wood314@gmail.com)

²Lightning and Space Effects, National Technical Systems, USA

I. INTRODUCTION

Electron emission of carbon nanotube (CNT) forests grown on silicon substrates was measured to investigate possible electron yield suppression due to the composition and morphology of CNT forests. CNT forests are vertically-oriented tubular formations of graphitic carbon grown on a substrate; these have been widely investigated for their extreme properties in optical, electrical, and mechanical aspects of physics and material sciences. CNT coatings are good candidates for yield reduction, in analogy with the near-ideal blackbody optical properties of CNT forests. Carbon with its low atomic number has an inherent low yield due to its low density of bulk electrons. Furthermore, the large aspect ratio of the vertically-aligned CNT allows for easy penetration of the high energy incident electrons, but enhanced recapture of lower-energy secondary electrons due to their wider angular distribution of emission. Total (TEY), secondary (SEY) and backscattered (BSEY) yield curves using 15 eV to 30 keV electron beams, along with energy emission spectra, were acquired for three CNT forest samples to determine the extent of yield suppression of the substrate due to the CNT forests [Wood, 2018].

II. SAMPLE GROWTH AND CHARACTERIZATION

CNT forests were made in the Utah State University Nanofabrication Lab using a non-plasma enhanced wet injection chemical vapor deposition method, utilizing a chemical precursor of xylene and ferrocene injected into the furnace held at 700 °C [Wood,2015]. Hydrogen and argon carrier gas flow into the furnace at 50 sccm facilitated even distribution as iron atoms coalesce on the substrate to create catalyst particles for free carbons to develop rings, forming the nanotubes.

Forest height, density, and defects are the main aspects dictating morphology and the CNT forest's ability to suppress the yield of the underlying substrate. Duration of growth and precursor volume tend to determine the height of the forest, while the molar concentration of ferrocene in the precursor influences the density of the forest, with higher concentration producing denser forests but more defects. These factors were examined using scanning electron microscopy (SEM) [Figs. 1 (a-d)] and energy dispersive x-ray analysis (EDS) [Fig 1(e- f)].

Three CNT forests of varying height and density were created (see Table 1). Optical and gravimetric measurements consistently determined the CNF forests had between 3% to 5% of the areal density of bulk graphite. EDS of the AISi 132 CNT forest taken with 10 keV electrons show ~8% Si and <1% Fe concentration over the area covered by 27-32 μm high CNT, consistent with a 34 ± 4 electron penetration range for 10

keV electrons through a forest with 3.3% carbon density [Wilson, 2012].

III. THEORY AND EXPERIMENTAL SETUP

Electron yield is an energy-dependent measure of the interactions of incident electrons with a material and characterizes the number of electrons emitted per incident electron [Eq. (1)].

- Total electron yield σ (TEY) is defined as the ratio of emitted electron flux to incident flux,

$$\sigma = \frac{N_{out}^{e-}}{N_{in}^{e-}} = \frac{Q_{out}^{e-}}{Q_{in}^{e-}} \quad (1)$$

- Backscatter electron yield η (BSEY) describes electrons emitted from the material which originate from the incident beam; operationally BSE are defined as electrons with emission energies >50 eV.
- SE electron yield δ (SEY), describes emitted electrons which originate within the material and are excited through inelastic collisions involving the incident electrons; operationally SE are defined as electrons with emission energies <50 eV. SEY is the difference between TEY and BSEY [Eq. (2)].

$$\delta = \sigma - \eta \quad (2)$$

SE can be further separated into SE_1 electrons produced as primary electrons enter the sample and SE_2 as backscattered electrons leave the sample.

Absolute TEY and BSEY were measured using a fully-enclosed hemispherical grid retarding field analyzer (HGRFA) [Fig. 2], which accurately determines absolute yield ($<5\%$) since the encapsulating design captures almost all of the emitted electrons [Dennison, 2106; Hoffmann, 2012] Concentric hemispherical grids are used to energetically discriminate the collected electrons.

Yield from layered structures has been modeled by Wilson [Wilson, 2019a; 2019b]. Because the energy of secondary electrons is typically only a few eV with concomitant small range values, secondary electron excitation within the material is dominated by the properties of the surface layer. Backscattered electron contributions from underlying layers will be the driving mechanism whereby secondary electron generation can be enhanced or decreased by underlying materials. For multilayer materials the contribution of

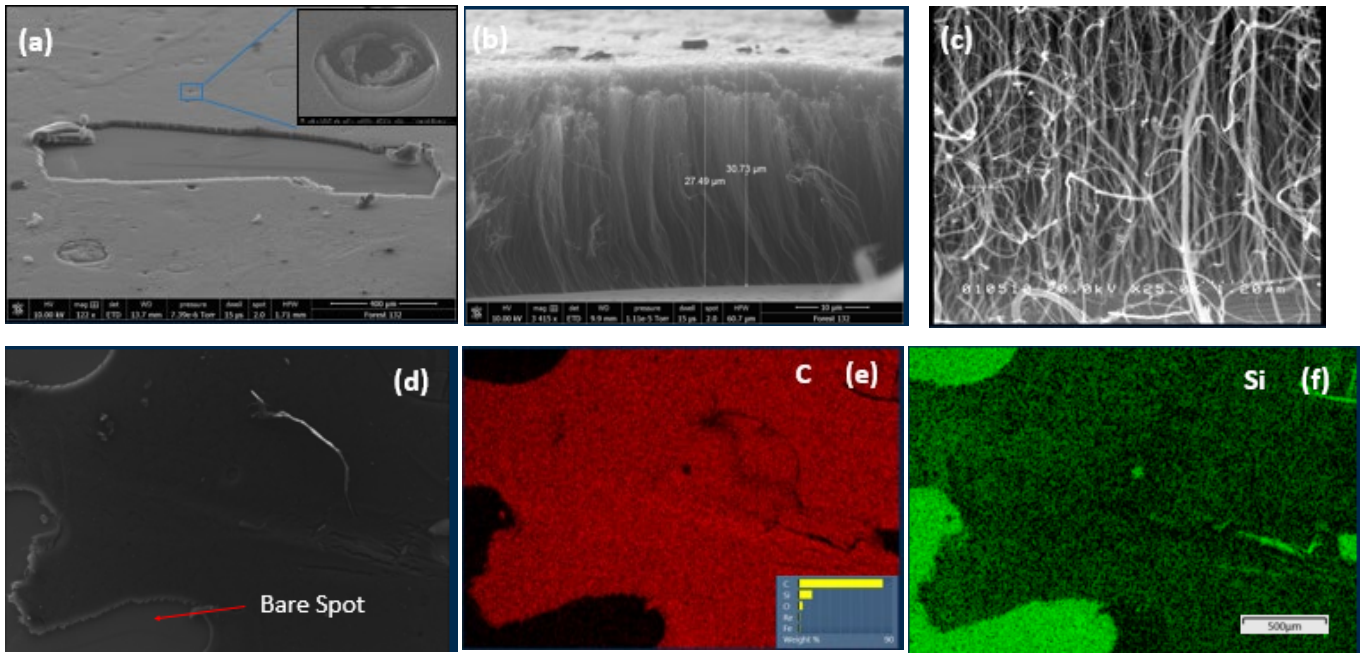


Fig. 1. Structure and composition of CNT forest samples. (a) Top view of CNT surface, with large void, smaller defects, and surface particles and inclusions visible. (b) Side view of AlSi 132 edge showing vertical alignment of CNT. (c) Close up view of CNT near their base on the AlSi substrate. SEM (d) and EDS (f and g) at 10 keV (e,f) of a AlSi 132, showing bare spots exposing Si substrate and composition of the CNT forest and substrate.

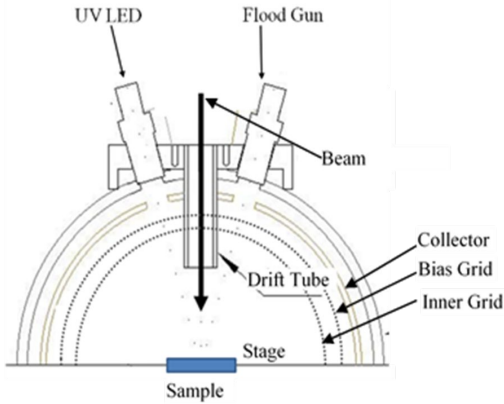


Fig. 2: Schematic of the hemispherical grid retarding field analyzer used to make absolute measurements of total and backscatter yields, allowing calculation of the secondary yield.

backscattered electrons from the underlying layers can only begin to contribute to the yield when the energy of the primary electrons becomes high enough such that their electron range is approximately twice the thickness of the surface layer [Wilson, 2019a].

III. RESULTS

Measurements of the TEY, SEY, BSEY, electron emission spectra were made over energy ranges of $30 \text{ eV} < E < 30 \text{ keV}$ as shown in Fig. 3.

- Fig 3(a) shows the SEY of the Si substrate with an Al diffusion barrier to be a weighted average of the yields of bulk Si and oxidized Al. As expected for the $\sim 3 \text{ nm}$ thin Al coating, the AlSi substrate yields are closer to those of Si than Al at higher energies.

Sample	Ferrocene (%)	Optical Surface Coverage (%)	Height (μm)	Effective Optical Density (μm)	Mass Density (mg/cm^3)	Fraction of Graphite Density
AlSi 127	0.5	(90 \pm 5)%	24-27	26 \pm 2	94 \pm 17	(4.1 \pm 0.8)%
AlSi 129	0.5	(91 \pm 5)%	42-51	47 \pm 6	129 \pm 13	(5.7 \pm 0.6)%
AlSi 132	0.2	(82 \pm 5)%	27-32	30 \pm 4	74 \pm 7	(3.3 \pm 0.3)%

- Fig. 3(b) compares SEY of the AlSi substrate, CNT forest AlSi 129, and HOPG (taken as a bulk surrogate for graphitic CNT).
 - Unlike the AlSi substrate, the yield of the CNT forest cannot be described as a simple combination of the AlSi substrate and graphitic carbon yields.
 - At $E > 4 \text{ keV}$ the CNT SEY approaches that of AlSi
 - At $1.2 \text{ keV} < E < 3 \text{ keV}$, the CNT forest yield is actually $\sim 10\%$ higher than the AlSi substrate. This is attributed to increased SE_2 production from the enhanced backscatter electrons from the AlSi substrate as they travel back out of the CNT forest.
 - At $600 \text{ eV} < E < 1200 \text{ eV}$, the CNT yield is between that of HOPG and AlSi, trending towards that of HOPG as the energy is reduced and SE_1 production becomes more dominate than SE_2 production from the AlSi substrate is overtaken by that of HOPG as the BSEY contribution from the substrate diminishes
 - At $E < 600 \text{ eV}$, the CNT yield of the forest is below that of *both* the AlSi substrate and HOPG. This is hypothesized as due to further suppression of low energy SE which are recaptured through CNT surface morphology effects (see Fig. 4)

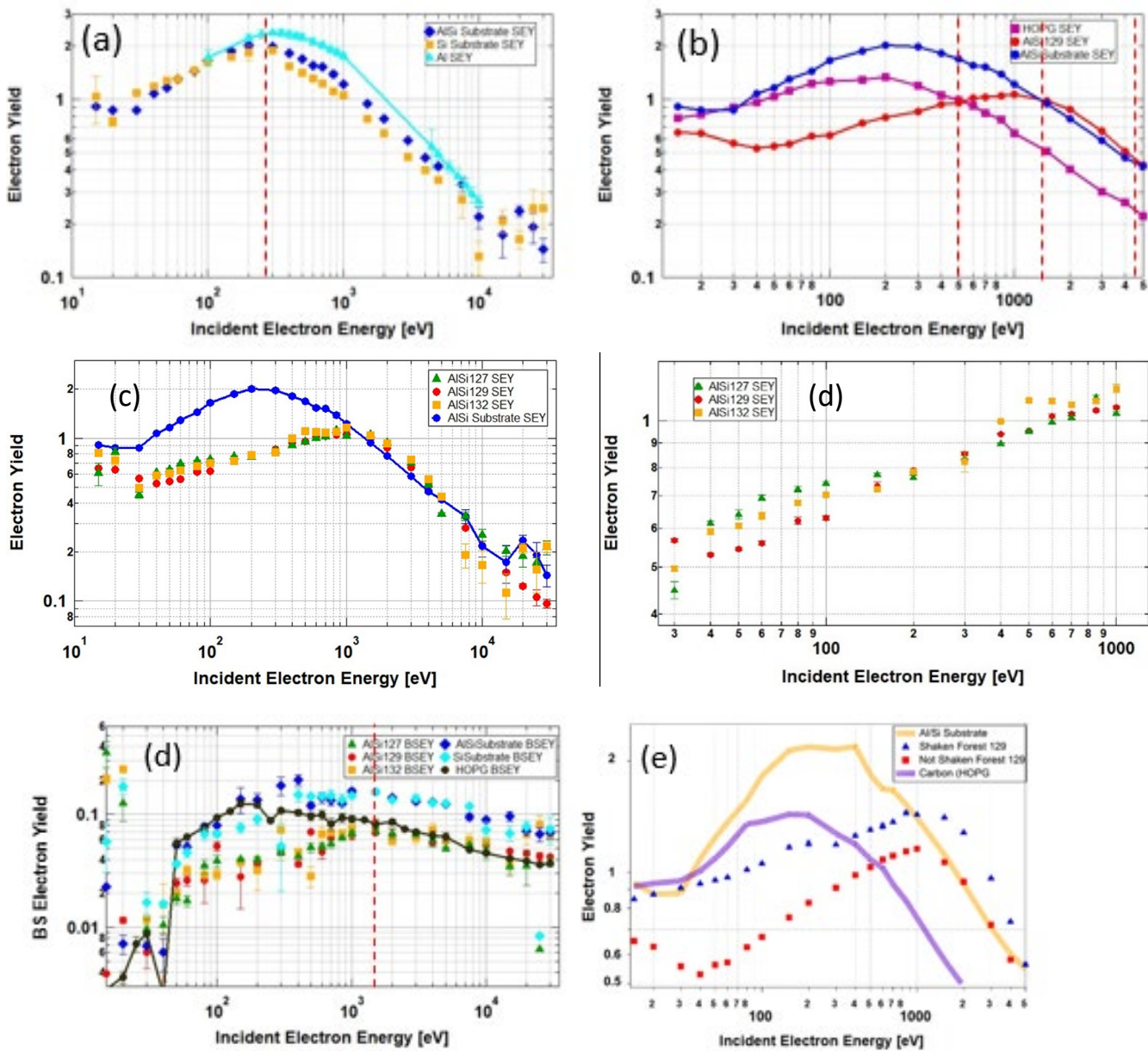


Fig. 3: (a) SEY yield curves of the AlSi substrate and its constituent bulk material, showing that the substrate is a direct near-linear contribution of its layered constituents. (b) Comparison of SEY curves of CNT forest sample AlSi129, bare substrate, and HOPG. This is not the case for AlSi 129 below ~600 eV (b), although above 1200 eV the yield of all the forests (c), is about 10% higher than even the substrate. (d) variance in yield among the forests only occurring between 30-100 eV, where the height of the forest seems to be the main factor in reducing the yield of the substrate. (e) BSEY versus energy for the CNT forest samples, uncoated substrate, and HOPG. (f) Comparison of SEY curves of shaken and unshaken CNT forest AlSi129 sample, bar substrate, and HOPG.

- Yields at $E < 30$ eV may not be reliable, due to sample charging and stray electric fields
- Fig. 3(c) compares the three CNT forests SEY with the substrate SEY.
- All of the CNT forest samples have strikingly similar SEY
- Slight differences in SEY at low energies among CNT samples (inset) suggest that the taller forest produces the largest morphology suppression due to CNT alignment
- There is very weak evidence that taller CNT samples extend the energy at which morphology suppression occurs
- Fig. 3(d) compares BSEY of the AlSi substrate, CNT forest AlSi 129, and HOPG
 - BSEY of all CNT forest samples are very similar
 - At $E > 1.5$ keV, CNT BSEY are very similar to HOPG and $>50\%$ less than BSEY for AlSi
 - At $E < 1.5$ keV, CNT BSEY is $\sim 50\%$ less than both HOPG and AlSi BSEY and displays the morphology suppression seen in SEY

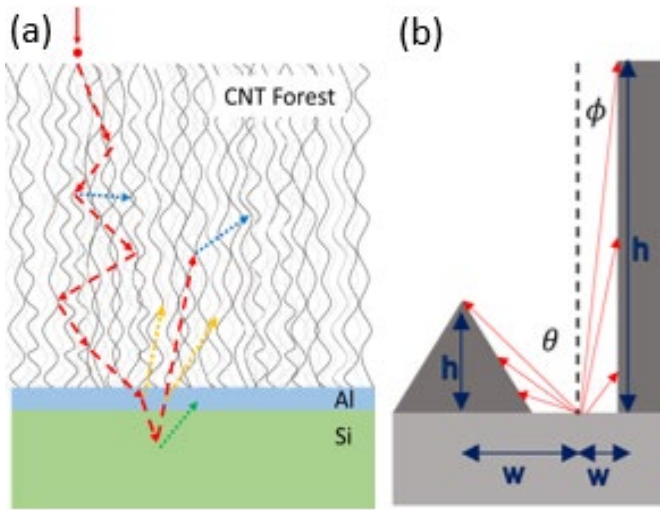


Fig. 4: (a) Possible scattering of both incident and backscatter electrons generating secondary electrons in various layers. (b) Schematic illustrating how surface protrusions and high aspect ratio, h/w , structures absorb emitted electrons. Low energy electrons with $\theta = \tan^{-1}(w/h)$ are recaptured.

- CNT samples subsequently subjected to violent shaking on a shaker table reduced yield suppression due to morphology, possibly as preferred vertical alignment of CNT is reduced [Lee, 2019]. See Fig. 5.
- Additional measurements are in progress of taller CNT samples (from $150 \mu\text{m}$ to $500 \mu\text{m}$) of similar density and vertical alignment to test the hypothesis that morphological suppression could be extended to higher energies $>3 \text{ keV}$ which could produce a CNT-coated substrate with uniform low SEY <0.5 over a very wide energy range.

REFERENCES

Dennison, J.R., et al., "Absolute Electron Emission Calibration: Round Robin Tests of Au and Polyimide," 14th Spacecraft Charging Tech. Conf., (ESA/ESTEC, Noordwijk, Netherlands, 2016).

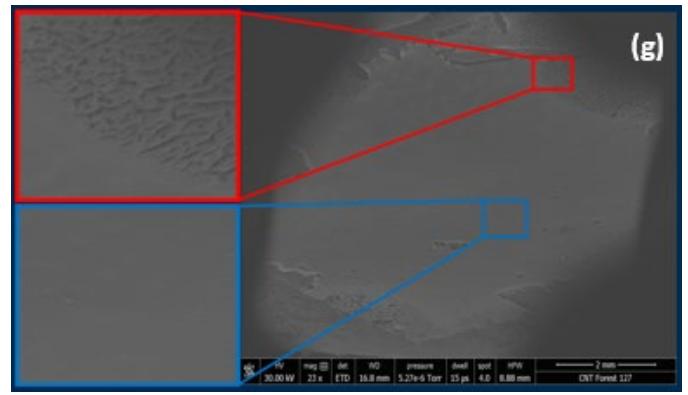


Fig. 5. Top view of shaken CNT sample showing (red) damage islands near the CNT forest edges and (blue) relatively undamaged regions in the sample center.

- Hoffmann, RC, and JR Dennison, "Methods to Determine Total Electron-Induced Electron Yields Over Broad Range of Conductive and Nonconductive Materials," IEEE Trans. on Plasma Sci., 40(2), 298-304 (2012).
- Lee, J., B. Wood, G. Wilson, T.C. Shen and JR Dennison, "Influence of Vibrationally-Induced Structural Changes on Carbon Nanotube Forests Suppression of Electron Yield," Applied Space Environments Conference 2019, (Los Angeles, CA, 2019).
- Wilson, G., and JR Dennison, "Approximation of Range in Materials as a Function of Incident Electron Energy," IEEE Trans. On Plasma Sci., 40(2), 291-297 (2012).
- Wilson, G., M. Robertson, J. Lee, and JR Dennison, "Electron Yield Measurements of Multilayer Conductive Materials," Applied Space Environments Conference 2019, (Los Angeles, CA, 2019a).
- Wilson, G., "Evolution of Internal Charge Distributions of Dynamic Multilayer Materials Due to Monoenergetic Electron Fluxes," PhD Thesis, Utah State Univ., Logan, UT, USA, 2019b.
- Wood, B.D., "Optical Characterization of Carbon Nanotube Forests," M.S. Thesis, Dept. of Physics, Utah State Univ., Logan, UT, USA, 2015.
- Wood, B.D., J. Christiansen, G. Wilson, T.C. Shen, and JR Dennison "Secondary Electron Yield Measurements of Carbon Nanotube Forests: Dependence on Morphology and Substrate," 15th Spacecraft Charging Tech. Conf., (Kobe, Japan, 2018).